

An empirical method for predicting extreme low winter sea ice extent in the Russian Arctic in the 21st century under global warming (on the example of the Barents Sea)

E. A. Cherenkova (cherenkova@igras.ru),
V. A. Semenov,
T. B. Titkova

Institute of Geography, Russian Academy of Sciences,
A.M. Obukhov Institute of Atmospheric Physics of Russian Academy of Sciences

ИНСТИТУТ ГЕОГРАФИИ
Российской академии наук



основан в 1918 году



Current climate in Arctic

- Higher rates of the warming in the Arctic relative to temperature changes in the middle and low latitudes (Arctic amplification) (e.g., [Bekryaev et al., 2010]) ;
- Transformation of atmospheric circulation regimes with an increased probability of stationary weather regimes and weather extremes [Francis&Vavrus, 2012; Semenov &Latif, 2015];
- Rapid reduction of the Arctic sea ice extent, which accelerated at the beginning of the 21st century [Ivanov et al., 2013; Semenov et al., 2015];
- The greatest loss of winter sea ice extent in the Barents Sea [Matveeva et al., 2020; Onarheim et al., 2015].

What is the future for sea ice extent?

Empirical assessments

the extrapolation of the current ice coverage trends in the Barents Sea into the future implies the ice-free conditions already in **2023** and **2036** for quadratic and linear trends, respectively [Onarheim and Årthun, 2017].

Climate model projections

the sea ice coverage in the Arctic have a significant intermodel spread:

- for example, ice-free conditions in the Barents Sea “are projected to occur for the first time in **2028** in GFDL CM3, **2061** in MPI-ESM-MR, and **2063** in NorESM1-M” [Onarheim and Årthun, 2017];

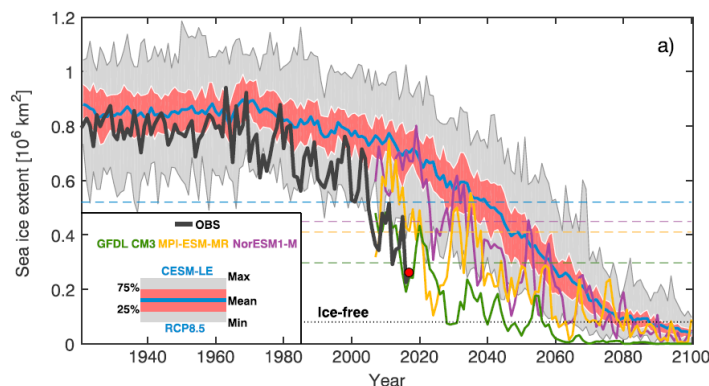


Figure. Past, present, and future winter Barents Sea ice extent in the (a) CESM-LE and (b) CESM-ME (ensemble mean: blue line; quartiles: red shading; ensemble spread: gray shading). The future sea ice extent (2007–2100) is also shown for GFDL CM3 (green), MPI-ESM-MR (yellow), and NorESM1-M (purple). Horizontal dashed lines illustrate the minimum sea ice extent for the corresponding preindustrial control simulations. Observed sea ice variability is shown in black, with the red dot highlighting the winter sea ice extent in 2017. Source: [Onarheim and Årthun, 2017]

- the models in average simulate ice-free conditions by the **end** of the **21st** century or around **2050** in the CMIP3 and CMIP5 ensembles, respectively” [Semenov et al., 2015].

However, “the Barents Sea is currently almost ice free in summer” [Semenov et al., 2015].

The **overestimation** of sea ice can be associated with an underestimation of the ocean heat transport to the Barents Sea in CMIP5 models [Li et al., 2017].



The goals of the study

- (1) to detect areas of the most significant linkage between sea ice concentration (SIC) in the Russian Arctic seas and surface air temperature (SAT) in the Northern Hemisphere in autumn, winter and spring during the period 1979-2019;
- (2) to determine the periods in which this linkage is the strongest;
- (3) to predict the timing of the ice free conditions in the Russian Arctic seas using statistical methods based on the observed link between sea ice concentration and surface air temperature over vast part of the Northern Hemisphere.

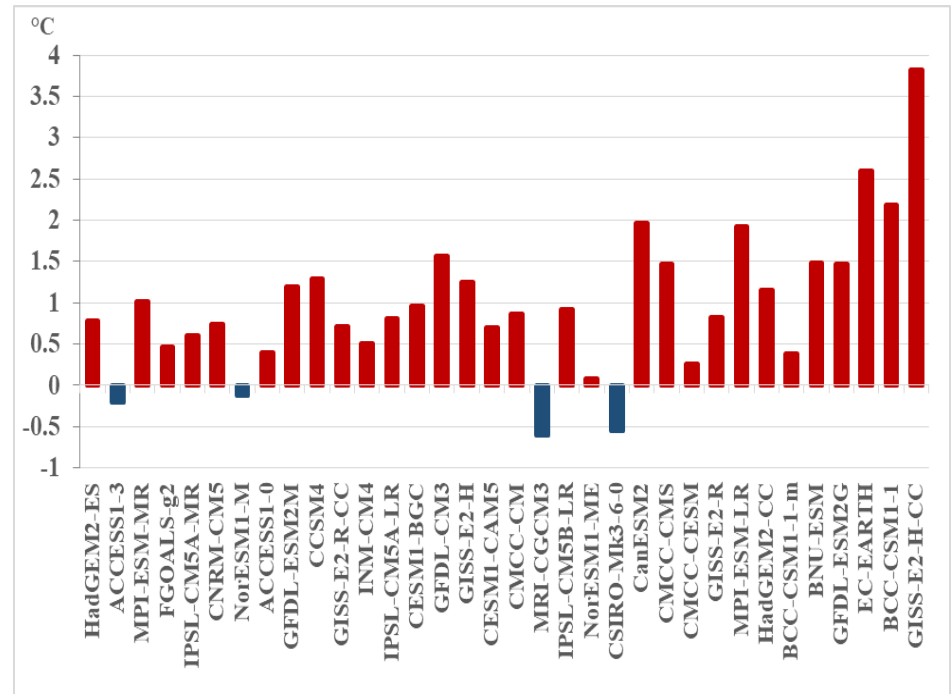
Data and methods

- The data of monthly SAT anomalies of the Northern hemisphere from datasets of NOAA GHCN v4 (meteorological stations) and ERSST v5 (ocean areas) with the spatial resolution of $2^{\circ} \times 2^{\circ}$, combined as described in [Lenssen et al., 2019].
- The data from the UK Met Office Hadley Center dataset (HadISST1.1) on monthly mean sea ice concentration in the Arctic with a spatial resolution of $1^{\circ} \times 1^{\circ}$ [Rayner et al., 2003].
- The data of numerical experiments with the global coupled atmosphere-ocean general circulation models (GCM) from CMIP5 (Coupled Model Intercomparison Project Phase 5) model ensemble from the global archive of the Center for Environmental Data Analysis [<http://data.ceda.ac.uk/>].
- The method of Singular Value Decomposition of covariance matrices (SVD) (Bretherton et al., 1992) was used to determine the areas of the most significant correlation between the leading modes of joint variability of the sea ice concentration (SIC) in the Arctic and the surface air temperature (SAT) of the Northern hemisphere to the north of 30° N in the autumn, winter and spring months in the 1979-2019 period.
- To explain the linkage between SAT and SIC, the regression model was designed based on the average values in the areas of the strongest correlation revealed by SVD analysis for the 1979-2019 period. The changes in SIC in the 21st century were calculated using the model parameters in the assumption that the found linkage between SAT and SIC will persist for several decades.

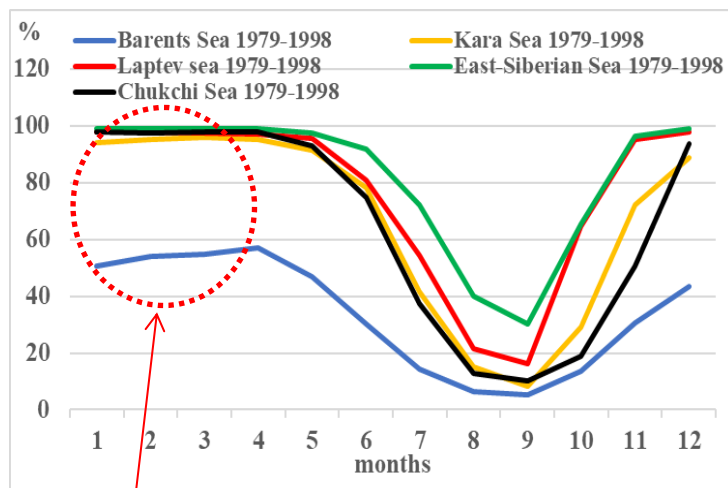


Simulation of the Surface Air Temperature by GCMs

- The most of the GCMs overestimate the SAT in November-January in the key areas in Scandinavia and over the Barents Sea during 1979-2019
- As the result, 30 GCMs out of 33 climate models were selected based on an estimate of minimum of the bias of different GCMs with regard to observed SAT in the same period



Changes in the concentration of sea ice in the Arctic seas of Russia in the period 1979-2019



The highest SIC in seasonal cycle in the seas of the Russian Arctic (January-March 1979-2019).

The difference in SIC (%) in the Russian Arctic between the 1999-2019 and 1979-1998 periods in January (1), February (2) and March (3):

region	Barents Sea			Kara Sea		
month	1	2	3	1	2	3
%	-15.1*	-16.3*	-11.4*	-5.01*	-3.6*	-1.8*
region	Laptev sea			East-Siberian Sea		
month	1	2	3	1	2	3
%	-0.08	0.09	0.25	0.33	0.2	0.13
region	Chukchi Sea					
month	1	2	3			
%	0.28	0.55	0.58			
* Significant changes						

- A significant decrease of the sea ice cover in January-March was observed in the Barents and Kara Seas in the 1999-2019 period compared to the 1979-1998 period;
- Sea ice cover shrank most rapidly in the Barents Sea (up to 16% per year);
- The rate of sea ice cover reduction in the Kara Sea did not exceed 5% per year so far;
- The increase in SIC in the remaining seas of the Russian Arctic in practically all months from January to March in the same period was insignificant (less than 1%).

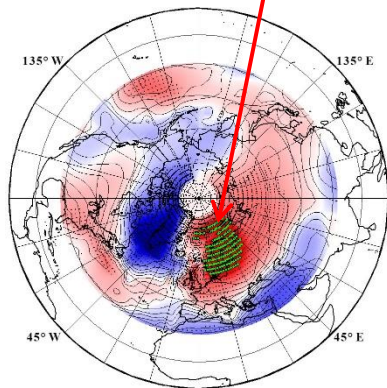
The linkage between the leading modes of joint variability of SIC in January-March and SAT in autumn, winter and spring in the period 1979-2019

- The linkage between SIC and SAT is robust for SIC in the Barents Sea in autumn, winter and spring.
- The most strongly related areas of the first leading mode of SVD analysis of joint variability of SAT in November-January and SIC in January-March;
- The spatial structure of the first leading mode of SVD analysis is represented by a zonal dipole highlighting changes in SAT and SIC of the opposite sign in the eastern and western regions of the Arctic (arctic dipole as possible mechanism);
- The most strongly related areas of:

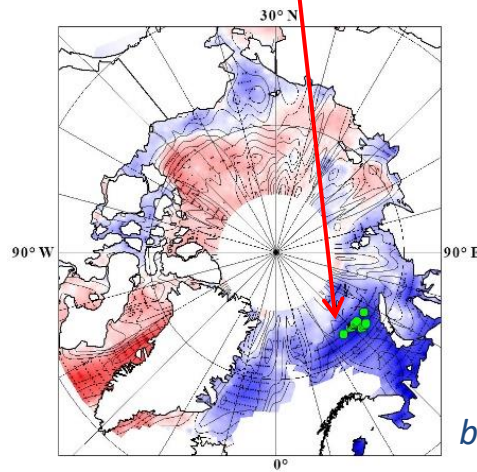
November-January SAT in Scandinavia and over the Barents Sea (inside the area indicated by green dots)

and

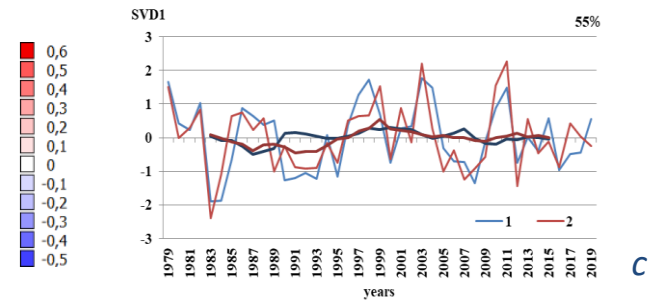
January-March SIC variability in the north of the Barents Sea (inside the area indicated by green dots)



a



b

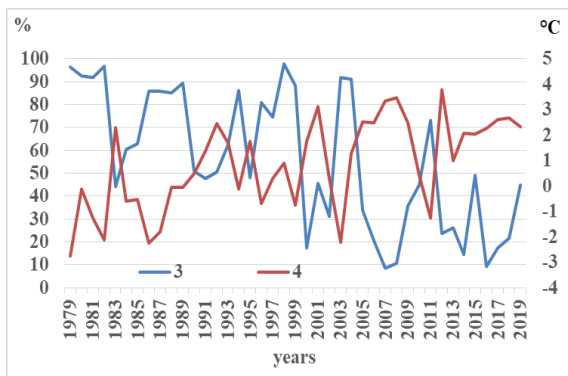


c

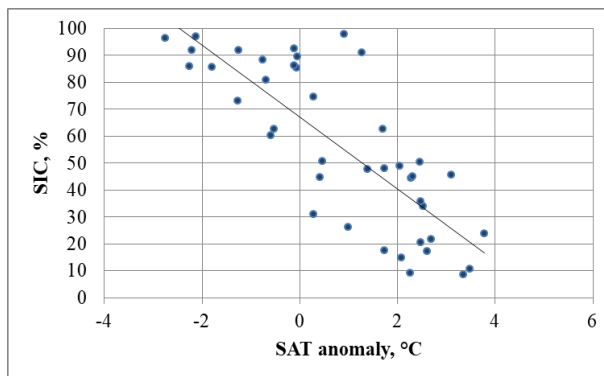
Figure. Spatial patterns (a, b) and time-series (c) of the first leading mode of SVD-analysis of observed SIC in the Arctic seas in January-March (1) and observed SAT in November-January (2) in the period 1979-2019.

The linkage between of January-March SIC the north of the Barents Sea and November-January SAT in Scandinavia and over the Barents Sea

Average January-March SIC in the north of the Barents Sea in the period 1979-2019 was strongly correlated with average November-January SAT in Scandinavia and over the Barents Sea (correlation coefficient is -0.8).



a



b

Figure. The variation of SIC in the north of the Barents Sea (3) and SAT anomalies in Scandinavia and over the Barents Sea (4) (a) and the linkage between SIC and SAT anomalies (b) during the period 1979-2019 in the areas of strong correlation between the leading modes of joint their variability of SIC and SAT.

The empirical linkage (described in table) between SIC in January-March in the north of the Barents Sea, SAT in November-January in Scandinavia and over the Barents Sea.

Table. The parameters of the regression model with SIC in January-March in the north of the Barents Sea as dependent variable and SAT in November-January in Scandinavia and over the Barents Sea as independent factor in 1979-2019.

model independent variable	regression coefficient	const	Std. Err.	t(30)	R ²	F	p-value
SAT	-13.3	67.1	1.6	-8.4	0.64	70	0.0000000003

The changes in ice concentration in the north of the Barents Sea in the current century based on modelled data

Based on the empirical linkage between SIC in January-March in the north of the Barents Sea, SAT in November-January in Scandinavia and over the Barents Sea in the late 20th - early 21st centuries, and the changes in SAT according to the climate model projections, the expected changes in ice concentration were estimated for north of the Barents Sea up to the end of the 21st century.

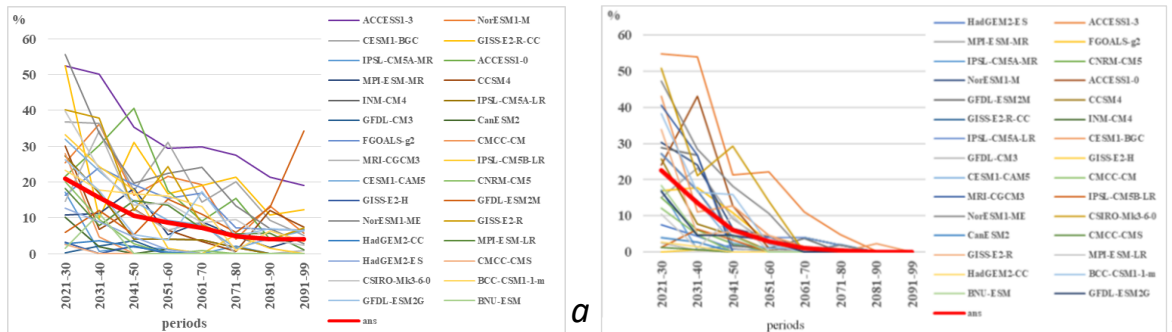


Figure. SIC averaged over different decades during the 21st century in the northern part of the Barents Sea in the period 2021-2099 based on GCMs data and their ensemble according to the RCP 4.5 (a) and RCP 8.5 (b) scenarios. The model ensemble mean is shown in bold red in figures a and b.

- The multimodel ensemble estimates of SIC based on the expected changes in SAT shows that the RCP 4.5 scenario assumes a reduction in the ice cover in the northern part of the Barents Sea in the period 2041-2050 to the values less than 10% (figure a). However, the complete disappearance of ice is not expected until the end of this century.
- According to the RCP 8.5 scenario, 10% SIC values in the region will be achieved approximately five years earlier than in the RCP 4.5 scenario, and almost complete sea ice removal should be expected by the middle of the 21st century (figure b).

The changes in ice concentration in the north of the Barents Sea in the current century based on HadGEM2-ES data

The proposed method of empirical linkage was applied to SAT data predicted by HadGEM2-ES and result was compared to SIC predicted by this climate model.

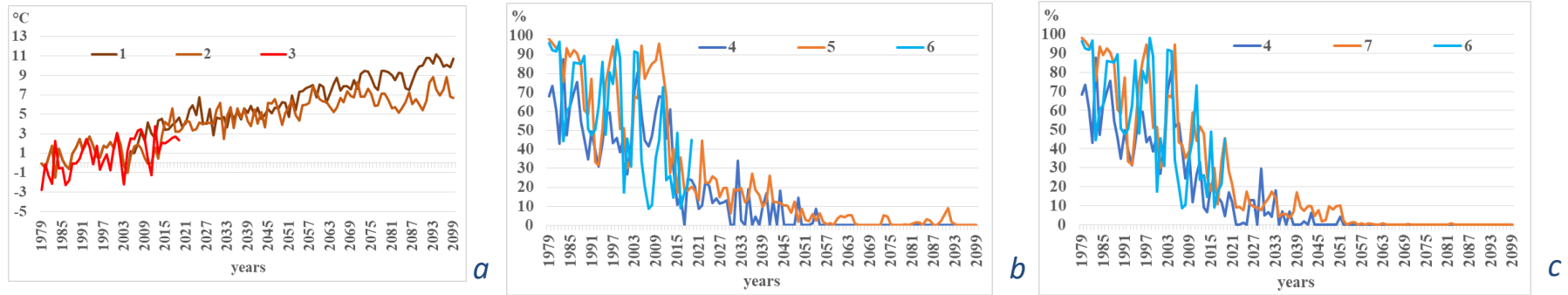


Figure. SAT anomalies in November-January in Scandinavia and over the Barents Sea (a) according to: HadGEM2-ES data (scenarios RCP 4.5 (1) and RCP 8.5 (2)) in the period 1979-2099 and HadISST1.1 (3) data in the period 1979-2019; SIC in January-March in the northern part of the Barents Sea (b) - (c) according to GISS-Temp data (6) in the period 1979-2019 and calculated by regression on SAT in the period 1979-2099 according to: HadISST1.1 data (4) and HadGEM2-ES data (scenarios RCP 4.5 (5) and RCP 8.5 (7)).

- According to the **RCP4.5** scenario and the revealed linkage between SAT and SIC in the last decades of the 20th century and the beginning of the 21st century, a warming of 5.2 °C in Scandinavia and over the Barents Sea in November-January (figure a) is expected to lead to the complete disappearance of ice cover in the north of the Barents Sea by the mid-2050s (figure b);
- the climate model assumes insignificant variability (less than 9%) in concentration in the second half of the 21st century (figure b);
- the warming by 5.5 °C in Scandinavia and over the Barents Sea in November-January in 2041-2050 under the **RCP 8.5** scenario is expected to lead to the complete ice disappearance in January-March in the north of the Barents Sea by the early 2050s according to the revealed linkage between SIC and SAT (figure c); a soon coming of year-round ice-free conditions in the Barents Sea;
- the **RCP 4.5** scenario assumes sharper than in **RCP 8.5** inter-annual fluctuations in sea ice concentration after 2022.



Conclusions

- The study of the leading modes of joint variability of the observed SIC in the Arctic and the SAT of the Northern hemisphere in the 1979-2019 period revealed the areas of the most strongly related January-March SIC in the northern part of the Barents Sea and November-January SAT in Scandinavia and over the Barents Sea.
- The link between SIC and SAT allows obtaining the semi-independent estimates of SIC in the northern part of the Barents Sea in the 21st century from an ensemble of 30 CMIP5 GCMs using models' SAT data.
- It was found that the RCP 4.5 scenario leads to a significant decrease of the sea ice in the northern part of the Barents Sea by the period 2041-2050. On the other hand, the complete disappearance of sea ice is not expected until the end of the century. Almost free-ice Barents Sea should be expected by the middle of the 21st century according to the most aggressive scenario RCP 8.5.



Appendix

- Singular Value Decomposition of covariance matrices (SVD) method. In general, according to the method, the covariance matrix $C(X, Y)$ of the time series of spatial vectors $X(t)$, $Y(t)$ can be represented by the following formula: $C(X, Y) = USV^T$, where S is the diagonal matrix of singular values, U is the unitary matrix of left singular vectors, V is the unitary matrix of right singular vectors. Singular Value Decomposition analysis method helps to reduce the dimension of the investigated links between time varying spatial fields and therefore to identify the leading modes that make the largest contribution to the explanation of the covariation variability. The heterogeneous correlation maps are associated with the coupled modes between the two parameters, i.e. the correlation between the temporal vector of one of parameters and time-series of the other field in each grid point. The spatial patterns of the results of the SVD analysis were obtained as the correlation of the matrix of each considered parameter with the corresponding SVD mode. The high correlation between averaged SAT and SIC over these areas reflects strength of a linkage.